Research Article GU J Sci, Part A, 11(3): 563-576 (2024) 10.54287/gujsa.1529271

Gazi University
Journal of Science
PART A: ENGINEERING AND INNOVATION
http://dergipark.org.tr/gujsa

Super Twisting Sliding Mode Control of Four-Phase Interleaved Boost Converter

Veli YENİL[1] Sadık ÖZDEMİR[2] Zafer ORTATEPE[3*]

[1] Department of Çardak OSB Vocational School, Pamukkale University, Denizli, Türkiye
[2] Department of Mechatronics Engineering, Pamukkale University, Denizli, Türkiye
[3] Department of Automotive Engineering, Pamukkale University, Denizli, Türkiye

Keywords

Fuel Cell
Interleaved Boost Converter
PI Control
Super Twisting Sliding Mode Control

Abstract

This paper presents a novel control method that integrates super-twisting sliding mode (STSM) voltage control with proportional-integral (PI) current control for a four-phase interleaved boost converter (IBC) in fuel cell applications. The STSM control, employed in the outer voltage loop, provides robust voltage regulation by generating precise reference currents for each phase. The conventional PI control in the inner current loop utilizes these reference currents to generate pulse width modulation (PWM) signals for each phase. The effectiveness of the proposed control strategy is evaluated through comprehensive simulation studies in MATLAB/Simulink, demonstrating an improvement in dynamic performance and enhanced robustness compared to conventional methods. Quantitative analysis shows that the output voltage quickly rises to the reference voltage within approximately 0.25 seconds in the proposed STSM-PI control method and improves transient response by 16 times compared to the conventional PI-PI method. This integrated STSM-PI control strategy offers significant advancements in reliability and efficiency making it a promising solution for high-performance fuel cell power systems.

Cite

Yenil, V., Özdemir, S., & Ortatepe, Z. (2024). Super Twisting Sliding Mode Control of Four-Phase Interleaved Boost Converter. *GU J Sci, Part A, 11*(3), 563-576. doi:10.54287/gujsa.1529271

Author ID (ORCID Number)

0000-0002-0257-5305 Veli YENİL
0000-0001-7676-7484 Sadık ÖZDEMİR
0000-0001-7771-1677 Zafer ORTATEPE

Article Process

Submission Date 07.08.2024
Revision Date 28.08.2024
Accepted Date 11.09.2024
Published Date 30.09.2024

1. INTRODUCTION

Fossil fuels, including coal, oil, and natural gas, have been extensively used across a wide range of applications for many decades. While fossil fuels have provided immense benefits in terms of energy access and economic development, their widespread use has also led to environmental and climate change concerns due to greenhouse gas emissions and other pollutants (Abas et al.; 2015; Eriksson & Gray, 2017). This has spurred efforts to transition towards more sustainable and cleaner energy sources and technologies that provide high-power efficiency and compactness.

Among these technologies, fuel cells have gained significant attention as an encouraging alternative. A fuel cell is a type of electrochemical device that uses a chemical reaction to transform chemical energy held in fuels into electrical energy. It operates similarly to a battery but does not require recharging; instead, it continues to produce electricity if it is supplied with fuel and an oxidizing agent (usually oxygen from the air) (Mekhilef et al., 2012). Fuel cells are known for their high efficiency, low emissions (since water is the primary by-product), and quiet operation. They have various applications including powering vehicles (fuel cell vehicles), and among all cleaner and sustainable energy sources, fuel cells are gaining more and more attention and becoming popular for electric transportation systems (Manoharan et al., 2019; Sazali et al., 2020).

However, the most important challenge in fuel cell technology is low output voltage, typically ranging between 0.5 to 0.8 volts per cell. This low output voltage is often insufficient for most applications, necessitating voltage

*Corresponding Author, e-mail: zortatepe@pau.edu.tr

conversion to higher voltage levels. Multiple fuel cells can be connected in series to achieve desired voltage levels, but this approach can reduce system reliability and add complexity (Hao et al., 2021). Thus, DC/DC boost converters have become essential in fuel cell systems to efficiently step up the voltage to a suitable level for end-use applications.

Conventional DC/DC boost converters are frequently used because to their simplicity and cost-effectiveness. However, they may suffer from low efficiency at low power levels, which is a common problem in fuel cell systems due to varying load demands. In addition, the inductors and capacitors used in conventional boost converters can be bulky and heavy, which is a significant drawback in applications where space and weight are critical, such as in automotive or portable fuel cell systems (Sagar Bhaskar et al., 2020).

Interleaved boost converter (IBC) offers a promising solution to these challenges by using multiple phases (or channels) of boost converters operating in parallel with interleaved switching signals. This design significantly reduces input and output ripple currents, enhances efficiency, and improves thermal management. By interleaving the switching phases, the converter minimizes electromagnetic interference (EMI) and reduces the size and cost of input and output filter components. Additionally, the IBC is scalable, allowing for higher power levels without significantly increasing the size of individual components. The reduction in ripple current also decreases conduction losses in the power switches and inductors, further enhancing overall efficiency (Seyezhai & Mathur, 2012; Khosroshahi et al., 2015; Mallikarjuna Reddy & Samuel, 2020).

To achieve optimal performance, various control methods have been introduced for IBC topology, including proportional-integral (PI) control, deadbeat control, sliding mode control (SMC), model predictive control (MPC) and super-twisting sliding mode (STSM) control (Kabalo et al., 2013; Nikhar et al., 2016). These control methods have different advantages related to fast dynamic response, energy efficiency and robustness.

In the SMC, the system is driven along a predefined sliding surface toward a desired state (Komurcugil et al., 2021). However, in practice, achieving and maintaining this sliding condition can be challenging in nonlinear systems (Sankar et al., 2021). STSM control is an extension of conventional SMC and a robust control technique used in nonlinear systems to achieve precise tracking performance (Gonzalez et al., 2012; Napole et al., 2021). Different from the SMC, the STSM control generates a second-order sliding motion along the sliding surface. This additional term helps in achieving faster convergence and smoother control action, even in highly nonlinear systems (Hao et al., 2023). Besides, the MPC is an effective nonlinear control method providing a fast dynamic response. Nevertheless, this approach has a chattering problem, and the MPC's performance is dependent on the system model (Schwenzer et al., 2021). Chattering can degrade system performance and lead to instability or reduced control accuracy. To decrease chattering effect, STSM control is applied to the different types of DC-DC converters (Hao et al., 2022; Guler et al., 2023).

In this paper, an integrated control method is proposed that combines STSM voltage control with conventional PI current control to enhance the robustness of four-phase IBC used in fuel cell applications. The STSM control ensures precise voltage regulation by generating accurate reference currents for each phase, while the PI control minimizes the error between the measured and reference inductor currents, ensuring equal current distribution across all phases. Proposed control strategy is thoroughly evaluated through simulation studies conducted in MATLAB/Simulink.

This study presents several contributions to show the superiority of the suggested topology over previous literature investigations and its application. The following can be used to summarize their contributions:

1. A combined STSM-PI control method is proposed and implemented to the IBC topology instead of conventional PI-PI control.

2. Thanks to the proposed control method, the chattering problem is reduced.

This article is organized as follows: Section 2 provides a detailed analysis of the four-phase IBC. Section 3 describes the proposed control scheme, including both STSM and conventional PI controls. Section 4 gives

the simulation results that verify the robustness of the control scheme. Finally, conclusion is given in Section 5.

2. ANALYSIS OF FOUR PHASE IBC

Four-phase IBC, as depicted in Figure 1, can be regarded as four conventional boost converters connected in parallel.

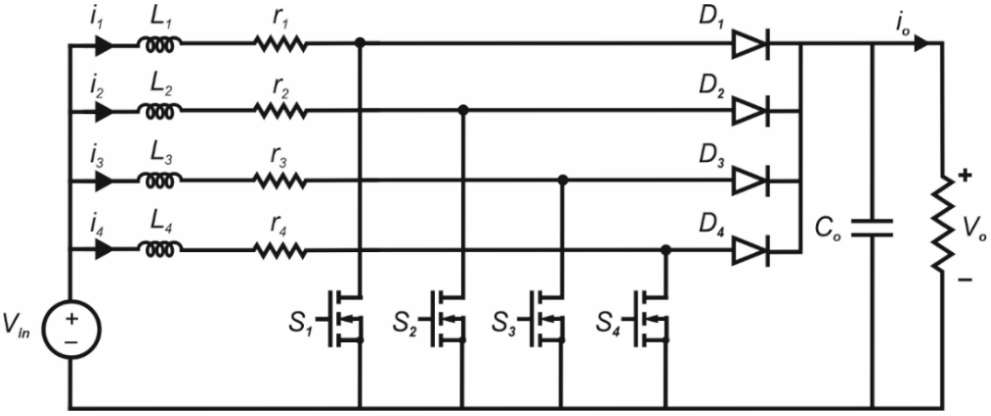

Figure 1. *Four-phase IBC topology*

In Figure 1, each boost converter has an inductor L_i $(i = 1, 2, 3, 4)$, a diode D_i $(i = 1, 2, 3, 4)$, a semiconductor switch S_i $(i = 1, 2, 3, 4)$, and an output capacitor (C_0). r_i $(i = 1, 2, 3, 4)$ denotes the parasitic resistance of each inductor. Besides, V_{in} denotes input voltage source, I_{in} denotes total input current, V_o denotes output voltage, I_o denotes output current, and R_o denotes load resistance. Four-phase IBC operates with continuous conduction mode (CCM), based on the drive signal of each converter.

A conventional boost converter has two operation modes. When the S_i is on, the input current of the inductor can be calculated with Equation (1). When the S_i is off, the capacitor and load are charged with the voltage source and inductor. Therefore, input current can be calculated with Equation (2).

$$\frac{di_{Li}}{dt} = \left(\frac{1}{L_i}\right)(V_{in} - R_o I_o) \tag{1}$$

$$\frac{di_{Li}}{dt} = \left(\frac{1}{L_i}\right)(V_{in} - R_o I_o - V_o) \tag{2}$$

By using Kirchoff's current law, the input current of the IBC can be obtained as follows:

$$i_{in} = i_{L1} + i_{L2} + i_{L3} + i_{L4} \tag{3}$$

By using Equation (1) and (2), the dynamic model of IBC can be obtained as follows:

$$\frac{di_{Li}}{dt} = \left(\frac{1}{L_i}\right)(V_{in} - (1 - d_i)V_o) \tag{4}$$

Where d_i (i=1,2,3,4) is duty cycle for the power switches.

$$d_i = \begin{cases} 0 & S_i\ is\ OFF\ state \\ 1 & S_i\ is\ ON\ state \end{cases} \tag{5}$$

The four-phase IBC model can be obtained using Kirchhoff's current/voltage law and the previously mentioned assumptions.

$$\frac{di_i}{dt} = -(1-d_i)\frac{v_o}{L} + \frac{r_L}{L}(v_{in} - i_i) \tag{6}$$

$$\frac{dv_o}{dt} = \frac{1}{C}\sum_{1}^{4} i_i - \frac{1}{f_L C}V_o - \frac{1}{C}\sum_{1}^{4} d_i i_i \tag{7}$$

Voltage gain of a four-phase IBC in CCM can be calculated as (8).

$$\frac{V_{out}}{V_{in}} = \frac{1}{1-D} \tag{8}$$

V_{out}, V_{in} and D are average DC values of V_o, V_{in} and d_i. Besides, the capacitor and inductor equations are given in (9).

$$\begin{cases} V_{in} - L_1 \dfrac{di_{L_1}(t)}{dt} = 0 \\ V_{in} - L_{2,3,4} \dfrac{di_{L_{2,3,4}}(t)}{dt} = V_o(t) \\ \displaystyle\sum_{i=2}^{4} i_{L_i}(t) - C\frac{dV_o(t)}{dt} = \frac{V_o(t)}{R} \end{cases} \tag{9}$$

2.1. Component Design

Inductors play a crucial role in energy storage and transfer process in a boost converter. In an IBC operating in continuous conduction mode (CCM), inductor current never falls to zero during the switching cycle, providing a continuous energy transfer to the output. The inductance value is calculated to provide that the converter operates in CCM, which minimizes current ripple and enhances efficiency. The inductance value (L) can be calculated using the following equation:

$$L = \frac{V_{in}D}{f_{sw}\Delta I_L} \tag{10}$$

where V_{in} denotes input voltage, D denotes duty cycle, f_{sw} denotes switching frequency and ΔI_L denotes peak-to-peak inductor current ripple. The effective inductance is divided among the phases for an interleaved converter. Therefore, the ripple current per phase is decreased, which allows for a smaller inductor size while maintaining the desired performance.

The output capacitor in an IBC is responsible for filtering the output voltage ripple and providing a stable DC output voltage. In CCM operation, the capacitor must be designed to handle the ripple current and maintain the desired output voltage. The capacitor value (C) is calculated based on the allowable output voltage ripple (ΔV_o), switching frequency, duty cycle and load current as follows:

$$C = \frac{I_o D}{f_{sw}\Delta V_o} \tag{11}$$

where I_o denotes output current, and ΔV_o denotes peak-to-peak output voltage ripple. Although a higher capacitance value reduces output voltage ripple, the circuit may become larger and more expensive. The ESR of the capacitor affects the output voltage ripple. Low ESR capacitors, such as tantalum or ceramic capacitors, are preferred to minimize the voltage ripple. The voltage ripple due to the ESR can be estimated as follows:

$$\Delta V_o = \Delta I_L \; x \; ESR \tag{12}$$

The choice of output diode is determined by reverse recovery time, voltage and current ratings. In addition to the V_o voltage, there needs to be a margin for the voltage value because of the ringing effect. Within the range

of the maximum output current, V_f should be as low as possible to reduce conduction losses. In order to reduce switching losses, the reverse recovery time (t_{rr}) must be as little as feasible.

3. CONTROL SCHEME

In this paper, the control scheme consists of two control methods. Voltage control loop is constructed with STSM, and a current control loop is constructed with conventional PI control. The objective of the STSM control is to provide good voltage tracking performance, and the objective of the conventional PI control is to minimize the error between the measured inductor current and reference values of inductor current, generated from the STSM voltage control loop. As a result, output voltage regulation and equal current for each phase are provided. The proposed control scheme is given in Figure 2.

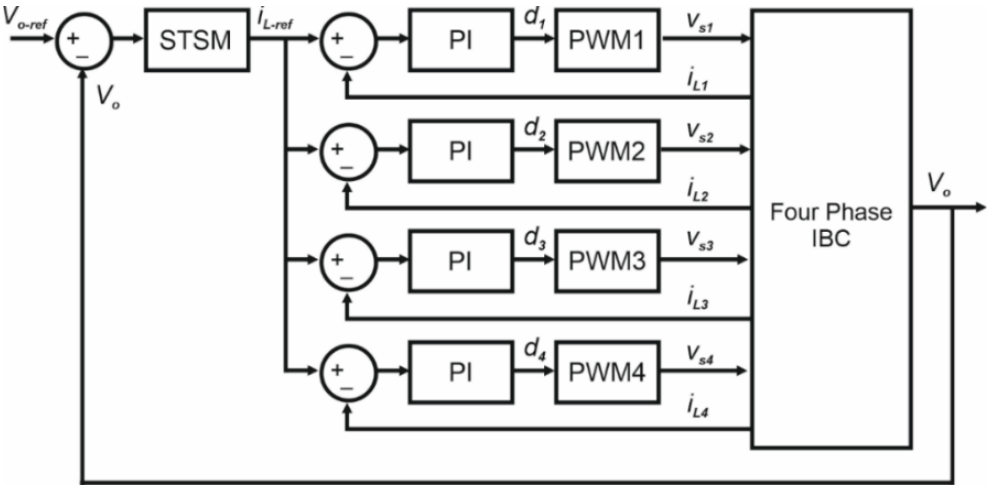

Figure 2. *Control scheme of four-phase IBC using STSM and PI control*

In four-phase IBC, each adjacent drive signals have a $T_s/4$ delay as given in Figure 3.

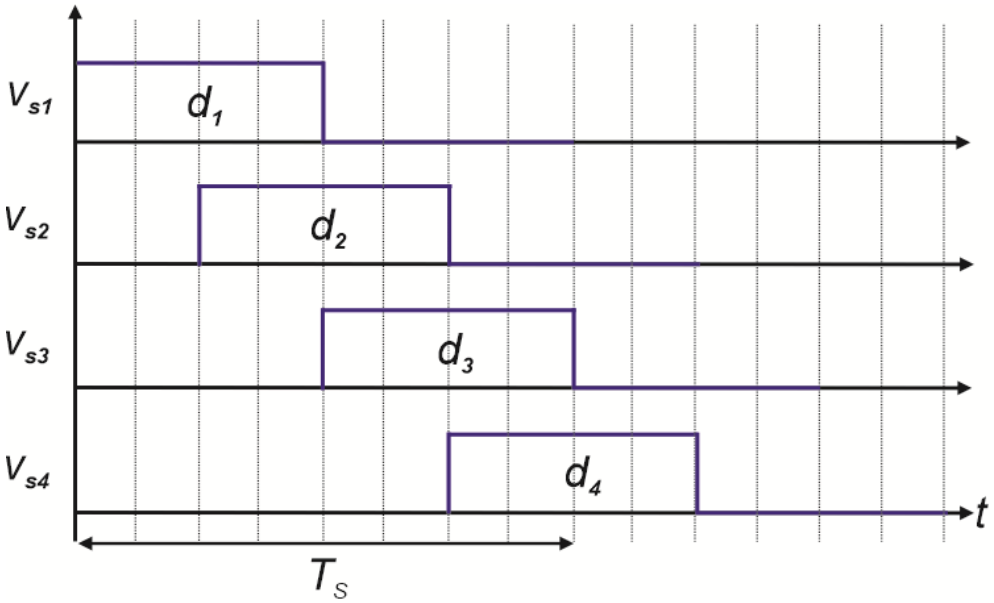

Figure 3. *Control signals of four-phase IBC*

In this paper, only CCM is considered in the simulation analysis. As shown in Figure 1, the proposed four-phase IBC topology contains four switches, diodes, and one capacitor. The transient states of the switches are ignored so, the switches have two switching states. "1" denotes on-state and "0" gives off-state. Table 1 gives the switching states of four-phase IBC topology, and S1000 says the S_1 switch is on-state and the rest of the switches are off-state.

Table 1. *Four-phase IBC operation modes*

Conditions		Switching States
Mode 1	$0 < d_1(t) + d_2(t) + d_3(t) + d_4(t) \leq 1$	S1000→S0000→S0100→S0000→S0010→S0000→S0001→S0000
Mode 2	$1 < d_1(t) + d_2(t) + d_3(t) + d_4(t) \leq 2$	S1000→S1100→S0100→S0110→S0010→S0011→S0001→S1001
Mode 3	$2 < d_1(t) + d_2(t) + d_3(t) + d_4(t) \leq 3$	S1011→S1001→S1101→S1100→S1110→S0110→S0111→S0011
Mode 4	$3 < d_1(t) + d_2(t) + d_3(t) + d_4(t) \leq 4$	S0111→S1111→S1011→S1111→S1101→S1111→S1110→S1111

3.1. Implementation of Super Twisting Sliding Mode (STSM) Control

The SMC is an effective nonlinear control method that is insensitive to system parameters. It has been widely used in power converter control. However, SMC has a chattering problem resulting in uncontrolled switching frequency. To reduce the chattering problem of conventional SMC, the STSM control can be implemented with different types of converters. To generate the inductor current reference, $i_{L_{ref}}$ for the IBC, the STSM control is selected and implemented in this paper. The STSM control block diagram is given in Figure 4.

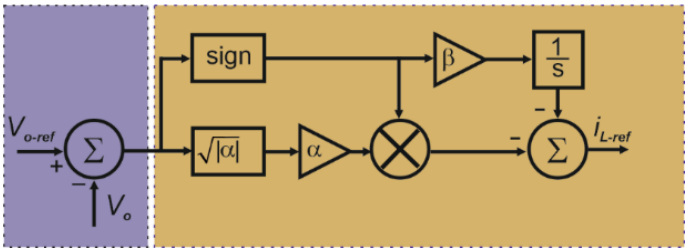

Figure 4. *STSM control method*

STSM control consists of two terms as equivalent control term (u_{eq}) and discontinuous control term (u_{st}):

$$u(t) = u_{eq}(t) + u_{st}(t) \tag{13}$$

$$u_{st}(t) = u_1(t) + u_2(t) \tag{14}$$

Also, the u_1 and u_2 can be calculated as follows:

$$\begin{cases} u_1(t) = -\alpha . sign(S) \\ u_2(t) = -\beta . |S|^{0.5} sign(S) \end{cases} \tag{15}$$

3..2 Implementation of Conventional PI Control

PI control is formed by combining proportional (P) and integral (I) controllers and is widely used in various power electronics applications due to its effectiveness, and simplicity and it is preferred to regulate current and voltage loops for the IBC. The proportional term provides an immediate response to the error signal. It is responsible for the speed of the transient response and helps to reduce the rise time. The integral term accumulates the error over time and eliminates steady-state error. It ensures that output voltage precisely matches the reference voltage in the steady state. Proper tuning of the proportional and integral gains (K_p and K_i) is crucial for optimal performance. PI controller effectively regulates the output voltage. Variations in input voltage or load are quickly corrected by adjusting the duty cycle. Interleaving of phases reduces the input and output current ripple, leading to smoother operation and lower electromagnetic interference (EMI). By distributing the load across multiple phases, the interleaved boost converter improves efficiency and reduces thermal stress on individual components. Theoretical equation of the PI controller is given in (16).

The block diagram of a conventional PI control is given in Figure 5. The controller compares the reference R(s) with the output control signal C(s) for having the error signal E(s). The error signal is minimized in the

PI controller then control signal U(s) is gained. Distortion signal D(s) and the control signal are added and employed to transfer function (plant, $G_p(s)$) to have the response signal.

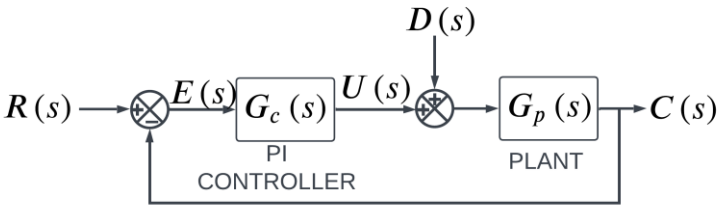

Figure 5. *Conventional PI controller block diagram*

$$G_c(s) = K_p + \frac{K_i}{s} \tag{16}$$

4. SIMULATION RESULTS

Simulation studies have been conducted using the MATLAB/Simulink platform in order to evaluate the control performance and dynamic response of the proposed control method. Figure 6 shows the block design of the simulation configuration and Table 2 contains a list of the simulation parameters.

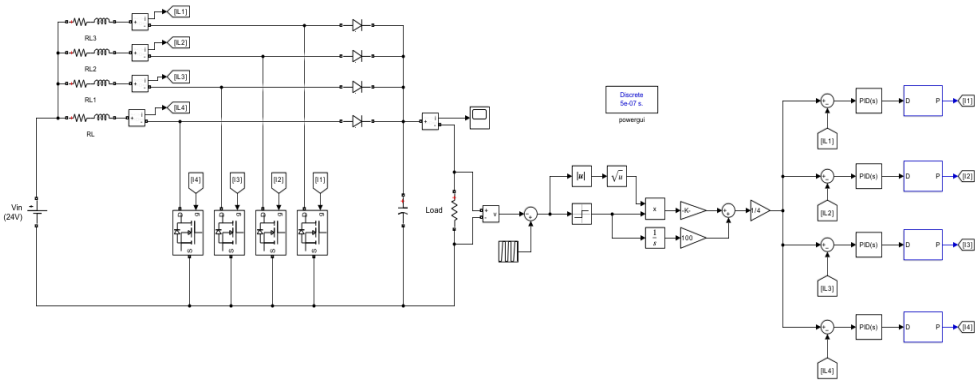

Figure 6. *Simulation layout of the system*

Table 2. *Simulation parameters*

Parameters	Symbol	Values
Input voltage	V_{in}	24 V
Load resistor	R_o	12 Ω
Inductor	L_i (i=1,..4)	500 µH
Inductor resistance	r_i (i=1,..4)	0.3 Ω
Output voltage	V_o	48 – 60 V
Output capacitor	C_o	1000 µF
Controller gains	α, β	100, 0.1
Controller gains	K_p, K_i	0.1, 10
Number of phases		4
Switching frequency	f_s	10 kHz

Figure 7 shows the output voltage performance of the proposed STSM-PI control method and conventional PI-PI control method, respectively. The controller gain (α and β) parameters of the proposed control method and the controller gain (K_p, K_i) parameters of PI controller are given in Table 2. In Figure 7, $V_{in} = 24V$ is applied to the input as a reference DC voltage. Also, $V_{o_{ref}} = 48V$ is applied as the reference output voltage until the 2. seconds. After 2 seconds, a reference ramp function ($V_{o_{ref}} = 48V\ to\ 60V$) is applied as a reference voltage, and after 3 seconds, $V_{o_{ref}} = 60V$ is applied constantly. In a transient state, maximum voltage ripple of the output voltage is measured as 2 % as shown in Figure 7a. It is also observed that even if the reference output voltage changes, the actual output voltage shows a good tracking performance in transient state and settles at the new reference after a few hundred milliseconds. Figure 7b shows the output voltage performance of the conventional PI-PI control method. The figure shows that the output voltage can never follow the reference voltage. As shown in the Figure 7 the proposed controller has better tracking performance under steady-state and transient responses compared to the conventional PI-PI control method.

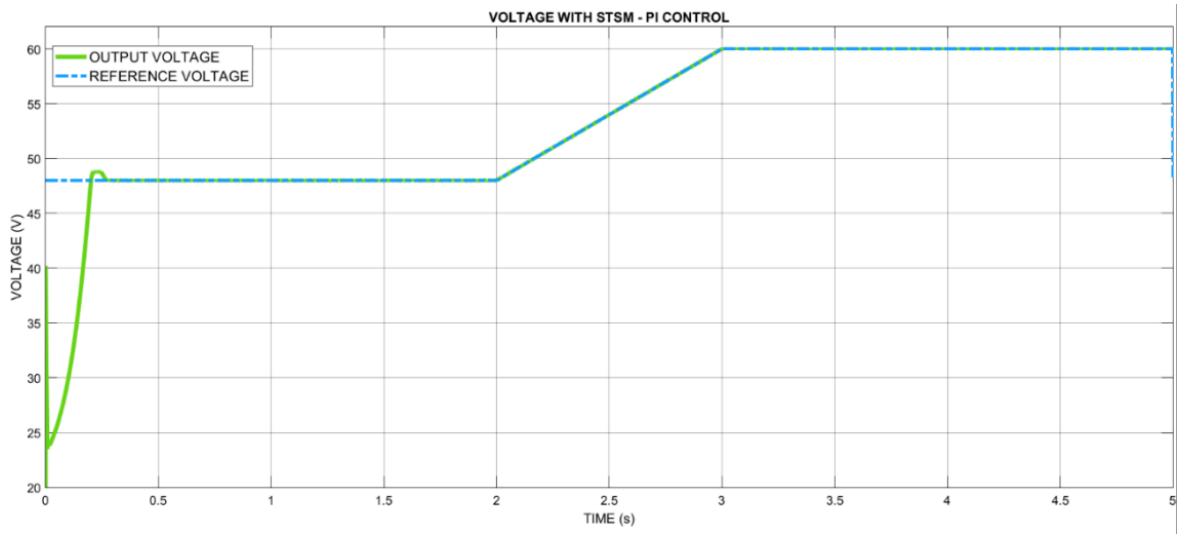

(a)

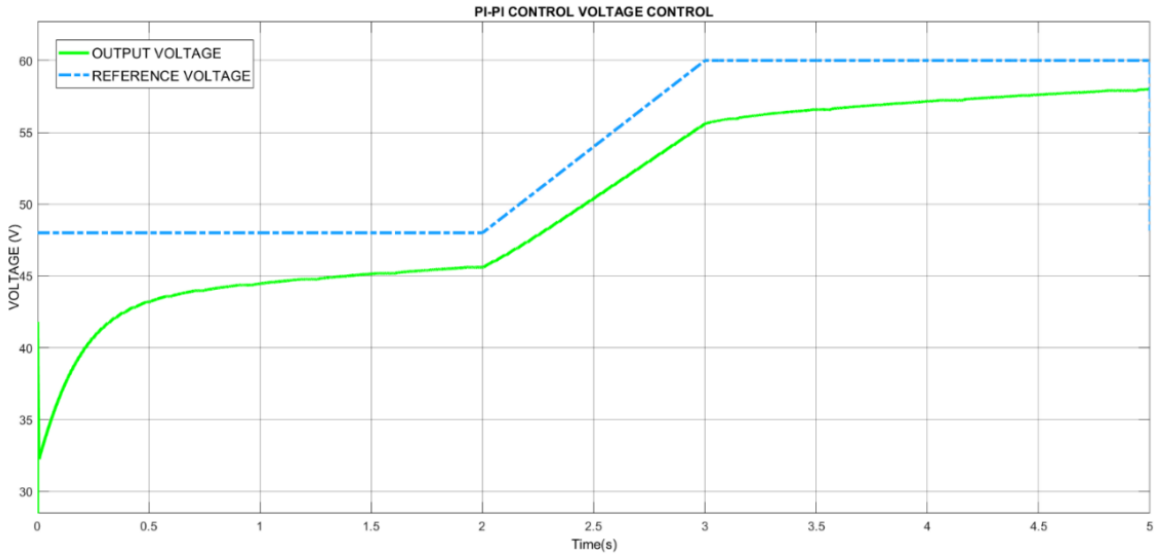

(b)

Figure 7. *The comparison of the output voltage performance* ***a)*** *Proposed STSM-PI controller,* ***b)*** *conventional PI-PI controller*

Figure 8 shows the output current performance of the proposed STSM-PI control method and conventional PI-PI control method, respectively. In Figure 8, $V_{in} = 24V$ is applied to the input as a reference DC voltage. Also, $V_{o_{ref}} = 48V$ is applied as the reference output voltage until the 2. seconds. After 2 seconds, a reference ramp

function ($V_{o_{ref}} = 48V\ to\ 60V$) is applied as a reference voltage, and after 3 seconds, $V_{o_{ref}} = 60V$ is applied constantly. As shown in the Figure 8a and 8b, the proposed controller has better output current tracking performance under steady-state and transient responses compared to the conventional PI-PI control method. The superior performance of the proposed method is mainly due to its high robustness to uncertainties and external disturbances in the system. This controller provided smoother control by minimizing the chattering effect while responding more efficiently and quickly to rapid changes in load current. Moreover, using the conventional PI-PI controller, the system is found to be less effective against nonlinear dynamics and large parameter variations, which resulted in slower and unstable load current reaching the desired reference values.

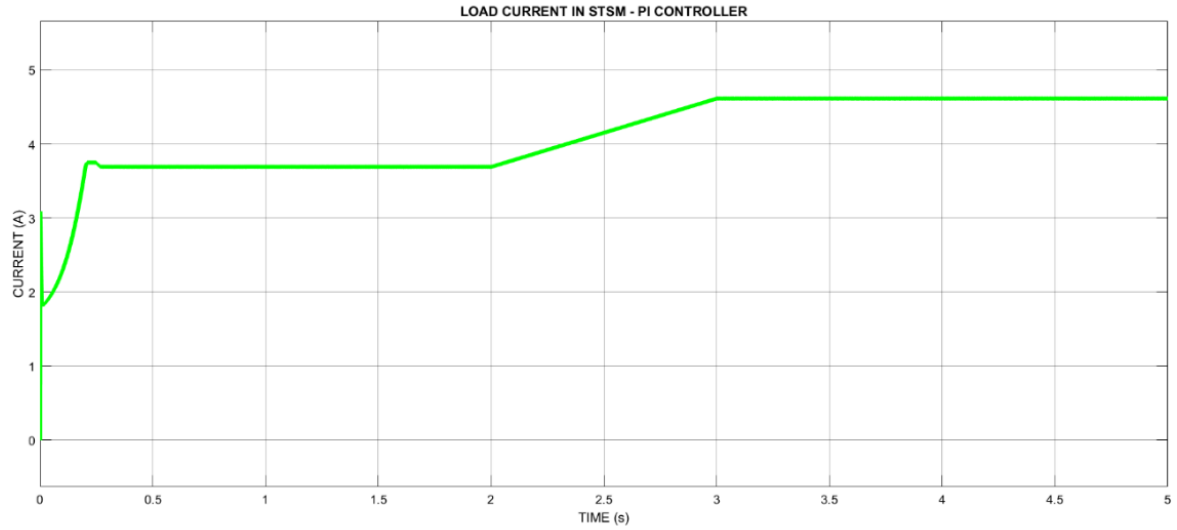

(a)

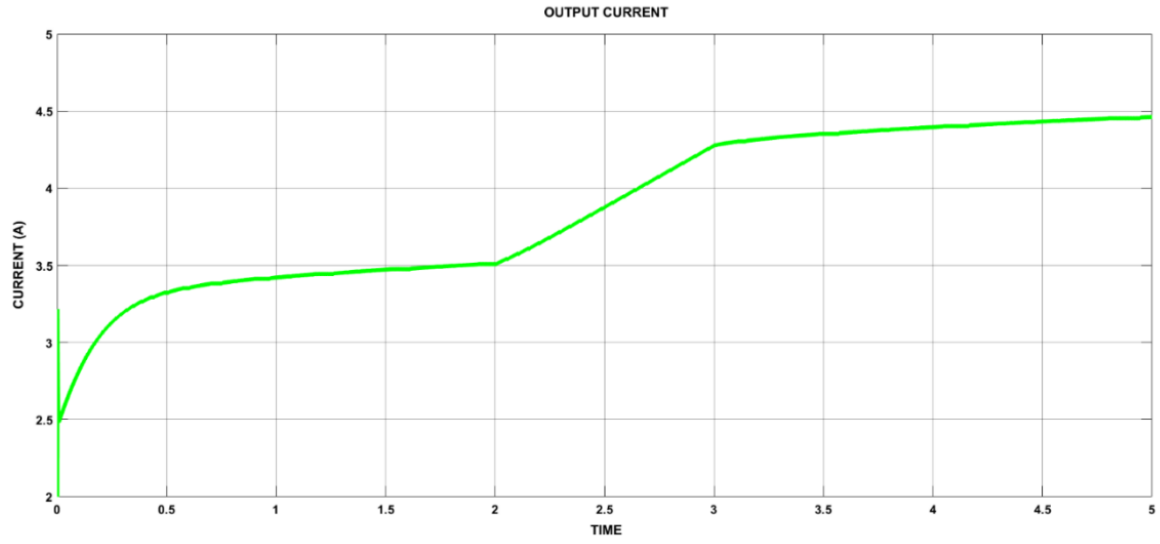

(b)

Figure 8. *The comparison of the output current performance* ***a)*** *Proposed STSM-PI controller,* ***b)*** *conventional PI-PI controller*

Besides, inductor currents of each phase and output current waveforms of the converter is given in Figure 9. As seen in the figure, the circuit operates in CCM mode since the phase currents never drop to zero. Also, from the figure it is seen that the total current is shared as phase currents.

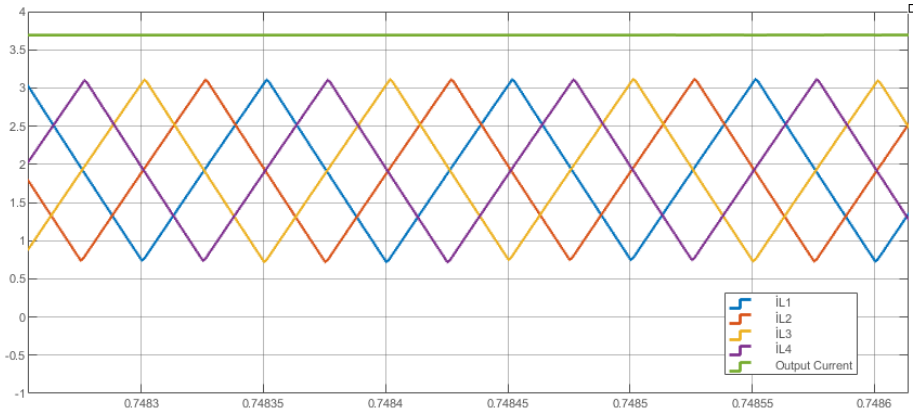

Figure 9. *Inductor currents and output current waveforms of the system*

Table 3 presents a comparative analysis of two control methods STSM-PI control and conventional PI-PI control based on several key performance characteristics: robustness, response time, stability, chattering, and complexity. The comparison in Table 3 shows that while the proposed STSM-PI controller offers superior performance in terms of robustness, response time, and stability, it does so at the cost of increased complexity and potential implementation challenges. In contrast, the conventional PI-PI controller is simpler and easier to implement but may not provide the same level of performance in dynamic or uncertain environments. The choice between these controllers depends on the specific requirements of the application, such as the need for fast response and high robustness versus the desire for simplicity and ease of implementation.

Table 3. *Comparison of proposed STSM-PI and conventional PI-PI controllers*

Characteristic	**STSM-PI Controller**	**PI-PI Controller**
Robustness	High	Low
Response Time	Fast	Moderate
Stability	High	Moderate
Chattering	Reduced	None
Complexity	Moderate	Low

Table 4 compares the proposed method with the existing studies. The proposed STSM-PI control method, while not the fastest in terms of settling time, offers a balanced performance with respect to voltage overshoot, and phase count. The four-phase topology ensures better current distribution and reduced ripple, while the discrete inductance design simplifies the implementation. 2% voltage overshoot is a reasonable trade-off, offering a balance between dynamic response and system stability. Compared to existing studies, the proposed method is competitive in terms of settling time, robustness, and reliability, especially when high efficiency and reduced ripple are important considerations.

Table 4. *Comparison of proposed method with the existing studies*

	Proposed	**(Zhuo et al., 2021)**	**(Alajmi et al., 2022)**	**(Banerjee et al., 2017)**	**(Nahar & Uddin, 2018)**
Number of phase	4	2	3	2	2
Inductance type	discrete	discrete	discrete	coupled	discrete
Voltage overshoot	% 2	none	none	%1.63	%30
Inductor current	CCM	CCM	DCM	CCM	CCM
Settling time	0.2 sec	0.1 sec	0.25 sec	0.02 sec	0.1 sec

4.1. Chattering Phenomenon

Chattering is a common issue in control systems, especially in conventional SMC. It causes to the rapid oscillations that occur around the desired trajectory or sliding surface. These oscillations are caused by the high-frequency switching actions inherent in SMC that are designed to keep the system state on the sliding surface. However, in practical applications, chattering can lead to several undesired effects, including increased wear and tear on mechanical components, reduced system efficiency and higher energy consumption. In some cases, chattering effect can also destabilize the system, making it challenging to achieve precise control.

MPC is a popular control strategy that predicts future behavior of the system based on a model and optimizes control inputs to achieve desired performance. While MPC is effective in providing fast dynamic responses, it can still suffer from chattering, particularly in systems with non-linearities or high-frequency dynamics. The root cause of chattering in MPC often lies in the discrete nature of the control systems and the approximation errors in the predictive model.

The STSM control, advance variant of SMC, is specifically designed to address the chattering issue. Unlike conventional SMC, STSM employs a second-order sliding mode approach. This approach includes two control terms: an equivalent control term and a discontinuous control term. The equivalent control term provides the system trajectory remains close to the sliding surface, while the discontinuous term is responsible for maintaining the system on the surface.

Consequently, STSM effectively addresses the chattering problem by introducing a second-order sliding mode that smooths the control action and reduces the frequency of switching. This contrasts with MPC, where chattering can still occur due to model mismatches and discrete control actions. The main advantage of STSM over conventional SMC and MPC lies in its ability to reduce or even eliminate chattering. This is achieved through the following mechanisms:

Second-Order Sliding Surface: STSM proposes a second-order sliding motion, which smooths out the control action, remarkably reducing the high-frequency switching that causes chattering. This second-order approach allows for a more gradual convergence to the sliding surface, minimizing the abrupt variations in control input that typically lead to chattering.

Robustness to nonlinearities and uncertainties: STSM is highly robust to external disturbances and system nonlinearities, which are often the source of chattering in other control methods. By accounting for these uncertainties within the control system, STSM can maintain stable performance without the need for excessive switching, further reducing chattering. This makes STSM particularly suitable for real-time applications where both computational efficiency and performance are critical.

5. CONCLUSION

In this paper, the performance of a four-phase IBC controlled by an integrated STSM and PI control strategy is thoroughly investigated. The primary objectives are to enhance the efficiency of the converter, improve transient response, and ensure robust performance under varying load and reference voltage conditions. Simulation results show that the proposed control method provides superior robustness against parameter variations, maintaining stability across a wide range of operating conditions. Quantitative analysis shows that the output voltage quickly rises to the reference voltage within approximately 0.25 seconds in the proposed STSM-PI control method and improves transient response by 16 times compared to the conventional PI-PI method. The STSM control also effectively minimizes the chattering effects, a common issue in conventional SMC, thereby enhancing overall system stability. The PI control, while simpler to implement, provides satisfactory steady-state performance with minimum steady-state error. Besides, the integrated STSM-PI approach outperforms the PI-PI control strategy in both dynamic and steady-state scenarios, making it a more reliable choice for high-performance fuel cell applications. These results suggest that the integrated control strategy is a viable solution for improving the efficiency and reliability of fuel cell power systems. Future work may focus on experimental validation to further confirm the simulation results and explore the application of this control strategy in real-world power electronic systems.

AUTHOR CONTRIBUTIONS

Conceptualization, V.Y.; methodology, V.Y. and S.Ö.; software, V.Y.; title, Z.O.; validation, V.Y., S.Ö. and Z.O.; research, S.Ö., and Z.O.; sources, S.Ö.; data curation, S.Ö.; manuscript-original draft, S.Ö.; manuscript-review and editing, Z.O.; visualization, Z.O.; supervision, Z.O. All authors have read and legally accepted the final version of the article published in the journal.

CONFLICT OF INTEREST

The authors declare no conflict of interest.

REFERENCES

Abas, N., Kalair, A., & Khan, N. (2015). Review of Fossil Fuels and Future Energy Technologies. *Futures*, *69*, 31-49. https://doi.org/10.1016/J.FUTURES.2015.03.003

Alajmi, B. N., Marei, M. I., Abdelsalam, I., & Ahmed, N. A. (2022). Multiphase Interleaved Converter Based on Cascaded Non-Inverting Buck-Boost Converter. *IEEE Access*, *10*, 42497-42506. https://doi.org/10.1109/ACCESS.2022.3168389

Banerjee, S., Ghosh, A., & Rana, N. (2017). An Improved Interleaved Boost Converter with PSO-Based Optimal Type-III Controller. *IEEE Journal of Emerging and Selected Topics in Power Electronics*, *5*(1), 323-337. https://doi.org/10.1109/JESTPE.2016.2608504

Sagar Bhaskar, M., Ramachandaramurthy, V. K., Padmanaban, S., Blaabjerg, F., Ionel, D. M., Mitolo, M., & Almakhles, D. (2020). Survey of DC-DC Non-Isolated Topologies for Unidirectional Power Flow in Fuel Cell Vehicles. *IEEE Access*, *8*, 178130-178166. https://doi.org/10.1109/ACCESS.2020.3027041

Eriksson, E. L. V., & Gray, E.MacA. (2017). Optimization and Integration of Hybrid Renewable Energy Hydrogen Fuel Cell Energy Systems – A Critical Review. *Applied Energy*, *202*, 348-364. https://doi.org/10.1016/J.APENERGY.2017.03.132

Gonzalez, T., Moreno, J. A., & Fridman, L. (2012). Variable Gain Super-Twisting Sliding Mode Control. *IEEE Transactions on Automatic Control*, *57*(8), 2100-2105. https://doi.org/10.1109/TAC.2011.2179878

Guler, N., Bayhan, S., Fesli, U., Blinov, A., & Vinnikov, D. (2023). Super Twisting Sliding Mode Control Strategy for Input Series Output Parallel Converters. *IEEE Access*, *11*, 107394-107403. https://doi.org/10.1109/ACCESS.2023.3320178

Hao, X., Salhi, I., Laghrouche, S., Ait-Amirat, Y., & Djerdir, A. (2021). Robust Control of Four-Phase Interleaved Boost Converter by Considering the Performance of PEM Fuel Cell Current. *International Journal of Hydrogen Energy*, *46*(78), 38827-38840. https://doi.org/10.1016/J.IJHYDENE.2021.09.132

Hao, X., Salhi, I., Laghrouche, S., Ait-Amirat, Y., & Djerdir, A. (2022). Backstepping Supertwisting Control of Four-Phase Interleaved Boost Converter for PEM Fuel Cell. *IEEE Transactions on Power Electronics*, *37*(7), 7858-7870. https://doi.org/10.1109/TPEL.2022.3149099

Hao, X., Salhi, I., Laghrouche, S., Ait Amirat, Y., & Djerdir, A. (2023). Multiple Inputs Multi-Phase Interleaved Boost Converter for Fuel Cell Systems Applications. *Renewable Energy*, *204*, 521-531. https://doi.org/10.1016/J.RENENE.2023.01.021

Kabalo, M., Paire, D., Blunier, B., Bouquain, D., Godoy Simões, M., & Miraoui, A. (2013). Experimental Evaluation of Four-Phase Floating Interleaved Boost Converter Design and Control for Fuel Cell Applications. *IET Power Electronics*, *6*(2), 215-226. https://doi.org/10.1049/IET-PEL.2012.0221

Khosroshahi, A., Abapour, M., & Sabahi, M. (2015). Reliability Evaluation of Conventional and Interleaved DC-DC Boost Converters. *IEEE Transactions on Power Electronics*, *30*(10), 5821-5828. https://doi.org/10.1109/TPEL.2014.2380829

Komurcugil, H., Biricik, S., Bayhan, S., & Zhang, Z. (2021). Sliding Mode Control: Overview of Its Applications in Power Converters. *IEEE Industrial Electronics Magazine*, *15*(1), 40-49. https://doi.org/10.1109/MIE.2020.2986165

Mallikarjuna Reddy, B., & Samuel, P. (2020). Analysis, Modelling and Implementation of Multi-Phase Single-Leg DC/DC Converter for Fuel Cell Hybrid Electric Vehicles. *International Journal of Modelling and Simulation*, *40*(4), 279-290. https://doi.org/10.1080/02286203.2019.1610689

Manoharan, Y., Hosseini, S. E., Butler, B., Alzhahrani, H., Senior, B. T. F., Ashuri, T., & Krohn, J. (2019). Hydrogen Fuel Cell Vehicles; Current Status and Future Prospect. *Applied Sciences*, *9*(11), 2296. https://doi.org/10.3390/APP9112296

Mekhilef, S., Saidur, R., & Safari, A. (2012). Comparative Study of Different Fuel Cell Technologies. *Renewable and Sustainable Energy Reviews*, *16*(1), 981-989. https://doi.org/10.1016/J.RSER.2011.09.020

Nahar, S., & Uddin, M. B. (2018, September 13-15). *Analysis the Performance of Interleaved Boost Converter*. In: Proceedings of the 4th International Conference on Electrical Engineering and Information and Communication Technology (ICEEiCT 2018) (pp. 547-551). Dhaka, Bangladesh. https://doi.org/10.1109/CEEICT.2018.8628104

Napole, C., Derbeli, M., & Barambones, O. (2021). A Global Integral Terminal Sliding Mode Control Based on a Novel Reaching Law for a Proton Exchange Membrane Fuel Cell System. *Applied Energy*, *301*, 117473. https://doi.org/10.1016/J.APENERGY.2021.117473

Nikhar, A. R., Apte, S. M., & Somalwar, R. (2016, December 22-24). *Review of Various Control Techniques for DC-DC Interleaved Boost Converters*. In: Proceedings of the International Conference on Global Trends in Signal Processing, Information Computing and Communication (ICGTSPICC 2016) (pp. 432-437). Jalgaon, India. https://doi.org/10.1109/ICGTSPICC.2016.7955340

Sankar, K., Saravanakumar, G., & Jana, A. K. (2021). Nonlinear Multivariable Control of an Integrated PEM Fuel Cell System with a DC-DC Boost Converter. *Chemical Engineering Research and Design*, *167*, 141-156. https://doi.org/10.1016/J.CHERD.2021.01.011

Sazali, N., Wan Salleh, W. N., Jamaludin, A. S., & Mhd Razali, M. N. (2020). New Perspectives on Fuel Cell Technology: A Brief Review. *Membranes*, *10*(5), 99. https://doi.org/10.3390/MEMBRANES10050099

Schwenzer, M., Ay, M., Bergs, T., & Abel, D. (2021). Review on Model Predictive Control: An Engineering Perspective. *The International Journal of Advanced Manufacturing Technology*, *117*(5-6), 1327-1349. https://doi.org/10.1007/S00170-021-07682-3

Seyezhai, R., & Mathur, B. L. (2012). Design and Implementation of Interleaved Boost Converter for Fuel Cell Systems. *International Journal of Hydrogen Energy*, *37*(4), 3897-3903. https://doi.org/10.1016/J.IJHYDENE.2011.09.082

Zhuo, S., Xu, L., Huangfu, Y., Gaillard, A., Paire, D., & Gao, F. (2021). Robust Adaptive Control of Interleaved Boost Converter for Fuel Cell Application. *IEEE Transactions on Industry Applications*, *57*(6), 6603-6610. https://doi.org/10.1109/TIA.2021.3113262

NOMENCLATURE

$\alpha - \beta$	Controller gains
C_o	Output capacitor
CCM	Continuous conduction mode
d_i	Duty cycles for the power switches
D_i	Diodes of the circuit
EMI	Electromagnetic interface
IBC	Interleaved boost converter
I_o	Output current
$i_{L_{ref}}$	Reference inductor current
K_p, K_i	Proportional and integral coefficients
L_i	Inductors of the circuit
MPC	Model predictive control
PI	Proportional-Integral
PWM	Pulse width modulation
r_i	Parasitic resistance
R_o	Resistive load
S_i	Power switches
SMC	Sliding mode control
$STSM$	Super-twisting sliding mode
V_i	Input voltage
V_o	Output voltage